



Experimental and Numerical Investigation on Micro-Bending of AISI 304 Sheet Metal Using a Low Power Nanosecond Laser

K. Paramasivan¹ · Sandip Das² ·
Sundar Marimuthu³ · Dipten Misra¹

Accepted: 21 February 2018 / Published online: 19 March 2018
© Springer Science+Business Media, LLC, part of Springer Nature 2018

Abstract The aim of this experimental study is to identify and characterize the response related to the effects of process parameters in terms of bending angle for micro-bending of AISI 304 sheet using a low power Nd:YVO₄ laser source. Numerical simulation is also carried out through a coupled thermo-mechanical formulation with finite element method using COMSOL MULTIPHYSICS. The developed numerical simulation indicates that bending is caused by temperature gradient mechanism in the present investigation involving laser micro-bending. The results of experiment indicate that bending angle increases with laser power, number of irradiations, and decreases with increase in scanning speed. Moreover, average bending angle increases with number of laser passes and edge effect, defined in terms of relative variation of bending angle (RBAV), decreases monotonically with the number of laser scans. The substrate is damaged over a width of about 80 μm due to the high temperatures experienced during laser forming at a low scanning speed.

Keywords Micro-bending · Finite element model · RBAV · Edge effect · Narrow HAZ

✉ K. Paramasivan
parma.gce@gmail.com

Sandip Das
sdas@mech.jdvu.ac.in

Sundar Marimuthu
marimuthusundar@gmail.com

Dipten Misra
dipten@gmail.com

¹ School of Laser Science & Engineering, Jadavpur University, Kolkata 700032, India

² Mechanical Engineering Department, Jadavpur University, Kolkata 700032, India

³ Manufacturing Technology Centre, Coventry CV7 9JU, UK

Introduction

Laser forming is a flexible technique that uses laser irradiation to generate a bending angle on components by exploiting residual thermal stresses induced by laser irradiation. A large number of experimental and numerical studies are performed in the past, to investigate the effects of process parameters on temperature distribution and deformation. Cheng et al. [1] presented the effects of geometry, including sheet width and sheet length on laser-induced deformation. They found that bending angle increases with the sheet dimension along the scanning path and sheet dimension across the scanning path has little effect on the bending angle. Venkadeshwaran et al. [2] used finite element simulation and response surface methodology to predict bending angle and optimise the process parameters for laser bending of stainless steel. Hoseinpour et al. [3] carried out statistical analysis to study effects of parameter on bending angle by FEM as well as experiment. Liu et al. [4] performed experimental studies on stainless foil for producing negative bending angles. It is reported that buckling mechanism (BM)-dominated laser parameters, such as larger ratio of beam diameter to specimen thickness and lower scanning speed, help to produce negative bending angles. Zahrani and Marasi [5] experimentally investigated the effects of process parameters on the edge effect and longitudinal distortion in laser bending process. Their results indicate that increasing sheet thickness, scanning speed and laser power and decreasing beam diameter lead to reduction of edge effect and longitudinal distortion responses. Shi et al. [6] performed numerical simulations to investigate deformation of a thin plate by choosing different process parameters. In this work, a detailed study is carried out on deformation of a plate, which is very useful to understand a high-precision forming process. Walczak et al. [7] discussed the sensitization of AISI 302 stainless steel on the basis of microstructural changes caused by temperature-induced phase transformations during low power laser forming. Ojeda and Grez [8] investigated laser forming of sheet metal using a raster scanned low output power CO₂ laser. They have suggested that by applying successive parallel scanning patterns, it would be possible to achieve a bending in the upward direction with certainty, which appears to be otherwise unpredictable for bending through buckling mechanism. Edwardson et al. [9] studied the variation in bending angle per pass during multi-pass TGM based laser process parameters.

Nowadays, many engineering products come in sizes of the order of microns. Therefore, the requirements of high accuracy in adjustment of component shapes have assumed greater importance. In place of using mechanical tools, laser beam can be suitably employed to achieve micro-bending or micro-adjustment of dimensions. A large number of studies are performed in the past on macro bending, to investigate the effects of process parameters on temperature distribution and deformation. However, it is necessary to conduct extensive studies on small scale deformations of sheet metals. Some of the investigations are explored related to micro-scale deformations. Chen et al. [10] studied deformation of stainless steel and ceramic specimens with precision of the order of nanometer using a pulsed Nd:YLF laser beam. Moreover, they carried out numerical simulations to understand the complex phenomena involved in pulsed-laser deformation process and to estimate the laser-induced temperature field, the residual stress field, and the deformation of the specimen. Zhang and Xu [11] studied high precision micro scale laser bending of ceramics, silicon, and stainless steel with the help of pulsed and CW lasers. They found that CW laser had produced more bending than pulsed laser and pulsed laser had caused much less change in surface composition and thermo mechanical damage to the

targets. Zhang and Xu [12] demonstrated a laser based technique to adjust curvatures of silicon micro cantilevers used for chemical and biological detection. Dirscherl et al. [13] presented theoretical and experimental investigations to study the effects of laser scanning speed, laser pulse energy and number of scans on high precision micro bending of different materials like copper, steel and silicon by ultrafast laser (femtosecond pulses) induced shockwaves. They have reported that ultrafast pulsed laser bending allows micro adjustment of a wide variety of materials without special pretreatment and micro adjustment can even be realized without spatial overlap. Ocana et al. [14] studied the effect of laser spot position in the workpiece on micro forming for a one-side pinned thin AISI 304 alloy with the help of a Q-switched Nd:YAG laser with nanosecond pulses. They reported that net bending angle increases as laser spot position is closer to 1/3 of the length and it decreases when laser spot is closer to the beam end. Hu et al. [15] carried out experimental investigations on laser peen forming of thin 1060 pure aluminium sheet in order to understand the effects of process parameters such as laser intensity, number of scans, scanning velocity on micro bending deformation. They found that the sheet metal can be made to bend not only towards the laser beam but also away from the laser beam depending on the specimen thickness and laser intensity. Moreover, the bending deformation can vary continuously and smoothly from the concave form to the convex by increasing the sheet thickness or decreasing the laser intensity. Griffiths et al. [16] presented the effects of pulse overlap, laser power, irradiation strategy and number of scans on net micro bending angle using picosecond laser pulses. They suggested that pulse repetition rate and, therefore, degree of pulse overlap must be larger to ensure sufficient buildup of temperature on the surface of the component for laser bending. Safari and Mostaan [17] presented experimental and numerical investigations of laser forming of cylindrical surfaces with arbitrary radius of curvature. To obtain a cylindrical surface with specific radius of curvature by laser forming, the number of parallel irradiation lines is the key parameter. Hence, they suggested the required number of irradiation lines for production of a cylindrical surface with a specific radius of curvature in their proposed analytical method. Moreover, they suggested that cylindrical surfaces with any radius of curvature can be produced easily with their proposed analytical method.

As can be seen from the literature review, most laser micro bending research focused on the effects of the basic laser process parameters on net bending deformations with ultrafast laser pulses which require availability of costly laser system. In the present work, experimental and numerical investigations are undertaken to study the micro bending behaviour of AISI 304 steel sheet using a low power Nd:YVO₄ laser source. Initially, a set of numerical simulations, using a finite element method, is carried out to develop a better understanding of the micro-bending process. Subsequently, a series of experiments have been performed to study the effects of process parameters on bending angle. Besides, the effect of number of scans on relative variation of bending angle (*RBAV*) along the free edge is also investigated. Moreover, a metallurgical investigation is conducted on laser formed AISI 304 specimens to study the effect of laser forming on surface morphology.

Experimental Procedure

AISI 304 sheet (70 mm × 40 mm × 0.8 mm) is chosen in this study. The sample is mounted on a table, with one end fixed and the other end free. The defocused laser beam is traversed

over it along the line 30 mm away from the fixed end of the plate. For all the experiments, the number of passes and the inter pass time are maintained constant at 20 and 12 s, respectively. Figure 1 shows the photographic view of the 12 W Nd:YVO₄ laser used in this study. The laser beam is focused to a diameter of 50 μm using a 195 mm telecentric lens. A laser displacement sensor (Make: Micro-Epsilon, Germany, Model: ILD 1300, Series: optoNCDT 1300) with an accuracy of 4 μm is used to measure the Z direction displacement at the free end of the specimen during the process.

Finite Element Simulation

The laser beam is modeled as a moving surface heat flux with small time increment. The total travel time of the laser beam is calculated based on the width of the plate and scanning speed of the laser beam. The time increment is calculated from total travel time and number of load steps. The model is meshed using free tetrahedral element for finite element simulation. A non-uniform mesh pattern is used to minimize the simulation time and memory requirement. Figure 2 shows, a typical mesh distribution used for the present simulation. The temperature dependent material properties are taken from [18, 19].

To develop a model for simulation of the laser forming process using the finite element method, following assumptions are made:

1. Material properties of the workpiece are isotropic.

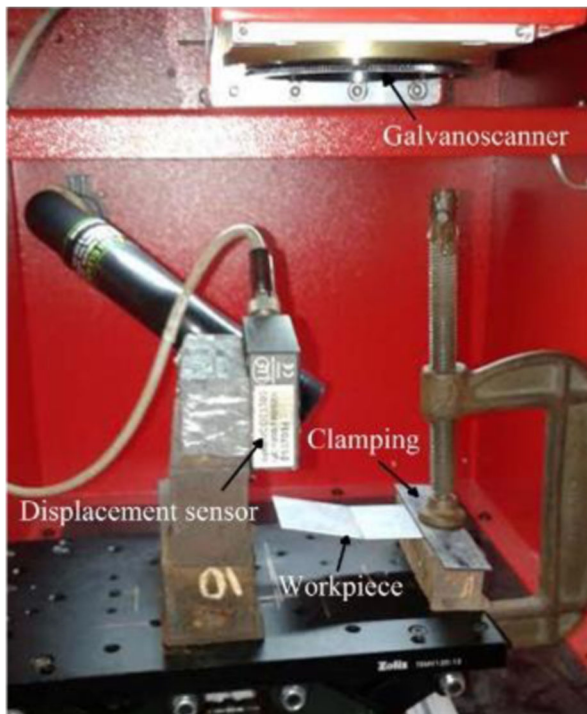


Fig. 1 Experimental set-up for laser bending

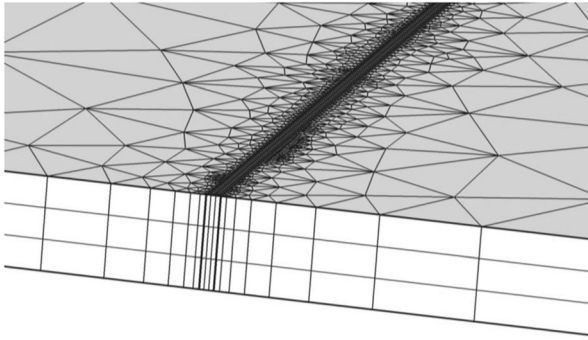


Fig. 2 Finite element mesh used for modeling

2. The distribution of laser intensity follows a Gaussian mode.
3. Within the workpiece, heat transfer takes place by conduction obeying Fourier's law and heat loss by free convection and radiation are considered from the surfaces of the sheet metal to the surrounding air.
4. von-Mises yield criterion is considered in the bending process.

Governing Equations and Boundary Conditions

Transient Thermal Analysis

In the present work, thermal linear elastic material model is used which combines linear elastic material with thermal expansion. During laser forming, the transient temperature field is calculated based on the mechanism of the heat conduction. The governing equation for heat conduction within the specimen can be written as follows:

$$\rho c \frac{\partial T(\mathbf{r}, t)}{\partial t} = k \nabla r \cdot (\nabla r T) \quad (1)$$

where, ρ is the material density (kg/m^3), c is the specific heat ($\text{J/kg}^\circ\text{C}$), k is the thermal conductivity ($\text{W/m}^\circ\text{C}$), $T(\mathbf{r}, t)$ is the temperature (K), \mathbf{r} is the coordinate in the reference configuration, t is time (s) and ∇r is the gradient operator.

The material cooling phase is made through natural convection and radiation from its surfaces exposed to ambience. The convection boundary condition can be expressed as follows:

$$q_{conv} = h(T_s - T_o) \quad (2)$$

where, h is the heat transfer coefficient, which is taken as ($10 \text{ W/m}^2 \text{ K}$), T_s is the sheet metal surface temperature and T_o is the ambient temperature, which is taken as 300 K.

The radiation boundary condition can be expressed as follows:

$$q_{rad} = \varepsilon \sigma (T_s^4 - T_o^4) \quad (3)$$

where, ε is the emissivity (set as 0.6) and σ is the Stefan Boltzmann constant ($5.6703 \times 10^{-8} \text{ W/m}^2 \text{ K}^4$).

Elasto-Plastic Analysis

The present simulation of the forming process accounts for the thermo-elasto-plastic deformation. So, total strain is assumed to be the summation of elastic, plastic and thermal components:

$$\varepsilon_{tot} = \varepsilon_e + \varepsilon_p + \varepsilon_t \quad (4)$$

where

ε_{tot} the total strain
 ε_e the elastic strain
 ε_p the plastic strain
 ε_t the thermal strain

The elastic strain vector is described by the elastic stress-strain relationship, which is defined as:

$$\{\varepsilon_{el}\} = [D]^{-1} \{\sigma\} \quad (5)$$

where

$$[D]^{-1} = \text{the elastic stiffness matrix} = \begin{bmatrix} \frac{1}{E} & \frac{-\nu}{E} & 0 \\ \frac{-\nu}{E} & \frac{1}{E} & 0 \\ 0 & 0 & \frac{1}{G} \end{bmatrix}$$

Plasticity of Material

Elastoplastic materials combine two principle types of behavior: elastic deformation, which is reversible deformation, and plastic deformation (or plasticity), which is irreversible and leaves a permanent deformation upon unloading. There are three elements in the plasticity theory: yield criterion, flow rule and hardening rule. The yield criterion determines the stress level at which yielding is initiated. For multi component stresses, it is characterised as a function of the individual components, $f(\{\sigma\})$, which can be interpreted as an equivalent stress σ_{eq} :

$$\sigma_{eq} = f(\{\sigma\}) \quad (6)$$

where

$\{\sigma\}$ stress vector

When the equivalent stress is equal to a material yield parameter σ_y ,

$$f(\{\sigma\}) = \sigma_y \quad (7)$$

The flow rule determines the direction of plastic straining and is given as:

$$d\varepsilon_{pl} = \lambda \left\{ \frac{\partial Y}{\partial \sigma} \right\} \quad (8)$$

where

- λ plastic multiplier (which determines the amount of plastic straining)
- Y function of stress termed the plastic potential (which determines the direction of plastic straining)

If Y is the yield function, the flow rule is termed associative and the plastic strain occurs in a direction normal to the yield surface.

The material hardened by plastic deformation can be described by two different types of behavior: isotropic hardening and kinematic hardening. In laser forming process, though every point of the work piece experiences a thermal cycle, the mechanical loading, however, as far as the plastic deformation is concerned, is essentially monotonic. Thus, the isotropic hardening rule is adopted. In the model, hardening of material is included by approximating stress-strain behaviour with a bi-linear curve.

$$\sigma_{ys} = \sigma_{ys0} + \frac{E_{Tiso}}{1 - \frac{E_{Tiso}}{E}} \cdot \varepsilon_{pe} \quad (9)$$

where

- σ_{ys} the current yield stress
- σ_{ys0} the initial yield stress and it represents the stress level where plastic deformation starts
- E_{Tiso} Isotropic tangent modulus
- ε_{pe} effective plastic strain
- E young's modulus and it is taken from the elastic material properties

Heat Flux

The moving heat flux Q produced by the laser beam, is applied on the top surface of the sheet metal. The moving heat flux considered for this study is a continuous mode. In this work, laser beam is assumed to have a Gaussian distribution and expressed as follows:

$$Q = \frac{2AP}{\pi R^2} \exp\left(-\frac{2r^2}{R^2}\right) \quad (10)$$

where, Q is the heat flux of the laser beam (W/m^2), A is the absorption coefficient, P is the laser power [W], R is the laser beam radius and r is the distance of a point from the centre of the laser beam.

Finite Element Simulation of the Laser Forming Process

In the present study, first, a set of numerical simulation using finite element method is carried out to get a better insight of the micro-bending process. Subsequently, a series of experiments have been performed to study the effects of process parameters on bending angle, edge undulation and morphological changes.

The results of Fig. 3a-d are presented for the case of a 40×10 mm sheet of 0.8 mm thickness. The values selected for the laser parameters are: 9 W power, 0.5 mm/s scanning speed, 1 number of pass and 50 μm beam diameter. Results corresponding to Fig. 3b, c refer to the centre point of the plate top surface.

Figure 3a shows the temperature variations at plate centres on the top and bottom surfaces having coordinates of (20, 5, 0.8) and (20, 5, 0), respectively, when the laser beam is moving along the mid-length of the plate. When the laser beam reaches the centre of the sheet, the temperature attains a maximum. When the laser beam moves

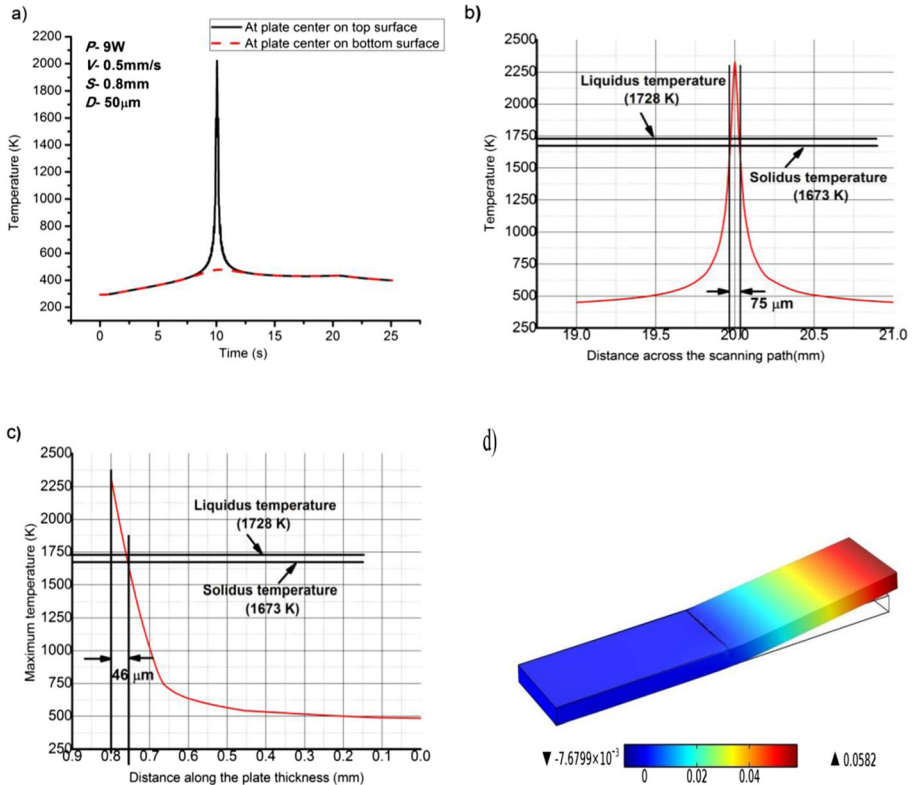


Fig. 3 Numerical simulation results of the bending process; **a** temperature variations at plate centre on top and bottom surfaces, **b** variation of temperature across the scanning path at plate centre, **c** variation of temperature through the plate thickness at plate centre, **d** z-component of displacement (mm) after one pass

away from the point, the temperature starts decreasing due to rapid cooling of the region. It can be seen from Fig. 3a that the temperatures at the centre point on top and bottom surfaces of the plate rise rapidly and attain maxima of 2324 K and 484 K, respectively. Fig. 3b presents variation of temperature across the scanning path during the laser beam irradiation. Figure 3c presents variation of temperature along the plate thickness during the laser beam irradiation. From Fig. 3c, it can be seen that the region spanning over a thickness of about 46 μm below top surface experiences complete melting as the temperature there reaches beyond the liquidus temperature. This is otherwise undesirable as bending will be less under such condition of local melting. This is due to very low scanning velocities and small diameter of the laser beam. As the travel speed of the laser beam is very low, the material heating and cooling rates takes place slowly. It results in high temperature on the top surface of plate and high gradient along the plate thickness direction as well. However, the maximum temperature at plate top surface reaches above material solidus temperature (1673 K). For this reason, locally a skin-depth region is damaged during laser irradiation. The damaged region is also evident from the experimental study, as can be seen from Fig. 13. However, at very low scanning speed and small beam diameter (0.5 mm/s, 50 μm) the damage is observed to be about 75 μm wide and 46 μm deep, which is very small and can be ignored. In this work, the substrate damage along the width and the depth is defined as the region which is heated to solidus temperature (1673 K) and beyond. The damage along the width and the depth is calculated from temperature results with respect to distances across the scanning line (x -direction) and through the plate thickness (z -direction). As can be seen in Fig. 3a, irradiation of the top surface by the laser beam causes a rapid increase in temperature, which leads to a high temperature gradient across the thickness. A large temperature difference of about 1840 K is set up between the top and the bottom surfaces. Consequently, bending is established through the temperature gradient mechanism.

Figure 4 shows the variation of bending angle with time at the mid-point of the free end having a coordinate (40, 5, 0.8). It can be seen from the figure, that bending angle increases during the laser heating process and remains fixed during the cooling time. In the beginning, a small counter bending is observed and a permanent bending angle of 0.166° is obtained at $t = 20.1$ s.

Figure 5 shows the stress distribution in X -direction at the centre of the top surface having a coordinate (20, 5, 0.8) which falls on the scanning path ($x = 20, z = 0.8$). It is observed from the results of numerical simulation that when the laser beam approaches the point under study, the nature of stress alters from tensile to compressive due to thermal expansion of the zone surrounding the point. When the laser beam reaches the selected centre point, the compressive stress attains a maximum. When the laser beam moves away from the point, the compressive stress starts decreasing due to rapid cooling of the region, and it changes to tensile stress due to the contraction of the surrounding material. The above description indicates that bending is caused by the plastic deformation induced by thermal stresses, and is strongly dependent on the transient temperature field and the coefficient of thermal expansion of the material under study. After the workpiece cools down completely to ambient temperature, residual stresses along the entire path of laser scan are tensile. The above stress pattern indicates that bending is caused by temperature gradient mechanism. For further investigation, a series of experiments are conducted to evaluate the influence of the

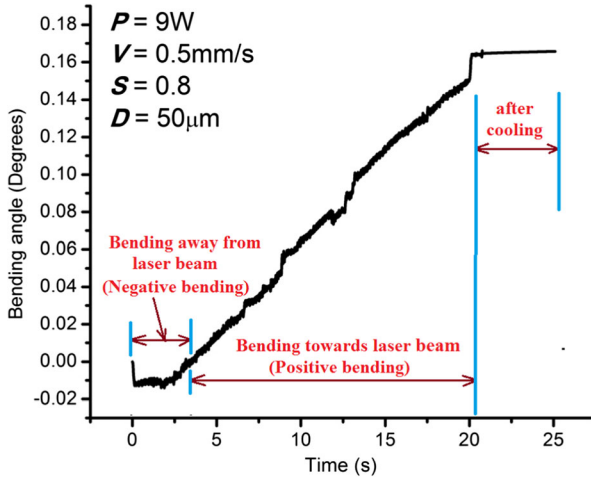


Fig. 4 Variation of bending angle with time at the middle of the free edge

variation of laser process parameters on the bending process. The laser parameters and the specimen dimensions, used in the present set of experiments, are listed in Table 1.

Result and Discussion from Experimental Investigation

Effect of Scanning Speed on Bending Angle

Figure 6 shows the effect of scanning speed on bending angle at different power. Bending angle decreases with increase in scanning speed. As scanning speed increases, the interaction time between the work piece and the laser beam decreases, resulting in

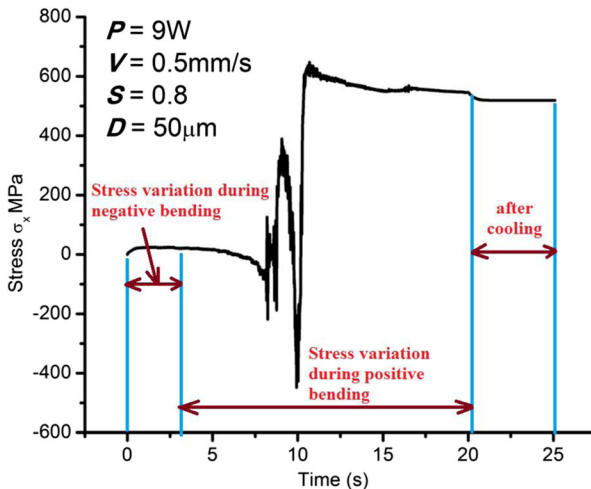


Fig. 5 Variation of X-component of stress with time at centre of the sheet (power = 9 W, scanning speed = 0.5 mm/s, plate thickness = 0.8 mm, beam diameter = 50 µm)

Table 1 Laser and specimen parameters used in experiments

| | | |
|---------------------|---------------|---------|
| Laser power | W | 7–9 |
| Scanning speed | mm/s | 0.5–2.5 |
| Laser beam diameter | μm | 50 |
| Number of scans | – | 20 |
| Specimen length | mm | 70 |
| Specimen width | mm | 40 |
| Specimen thickness | mm | 0.8 |

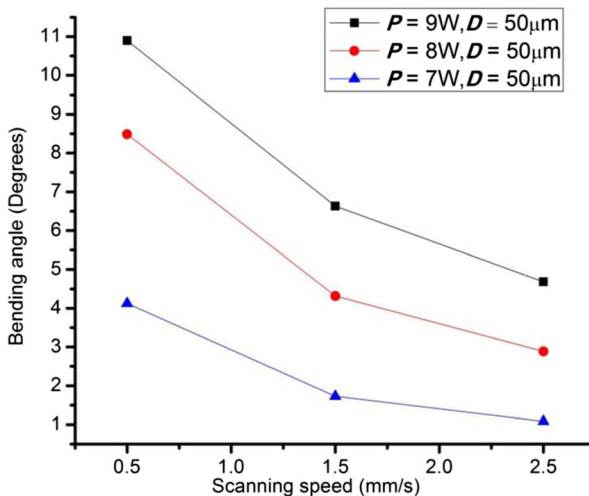
reduced absorption of heat by the work piece, lower peak temperature and lower plastic stress. Thus, the amount of bending decreases with increase in scanning speed.

Based on the experimental data, a regression Eq.(1) is developed, using least square method, to estimate bending angle as a function of laser process parameters (power and scanning speed) within the limits of laser micro-bending parameters considered in the present study.

$$\alpha_b = -42.9154 + 9.6772 \times P + 0.474 \times V - 0.7947 \times P \times V - 0.3713 \times P^2 + 1.1361 \times V^2 \quad (11)$$

The adequacy measures R^2 (0.995) and adjusted R^2 (0.993) are in reasonable agreement and are close to 1, which indicate adequacy of the model.

Figure 7 shows the relationship between the predicted and the experimental values of bending angle highlighting good agreement between the predicted results and the experimental data.

**Fig. 6** Effect of scanning speed on bending angle at different power (No. of pass = 20)

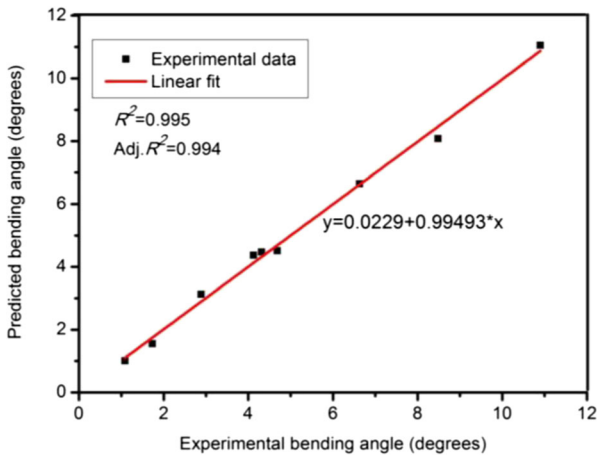


Fig. 7 Plot of predicted vs. actual response of bending angle results

Effect of Operating Distance on Bending Angle

Although considerable effort has gone into characterizing the laser forming process in terms of process parameters and conditions, the effects of operating distance (the distance of the scan line from the fixed edge) on bending angle has received very little attention. It is expected that the amount of bending changes with change in operating distance. In real time applications, the beam is expected to move not necessarily along the mid-line of the sheet. Figure 8 shows the variation of bending angle with operating distance. There is a reduction in bending angle when the operating distance is closer to the free edge. In the present case, there is only internal restraint offered by the bulk of unheated mass surrounding the heated zone and there is no external constraint, as the plate is fixed along one edge only. Hence, in the present case, in absence of external constraint, the magnitude of the final tensile stress and the consequent plastic strain depend mostly on the quantum of mass surrounding the heated zone. As the scan line

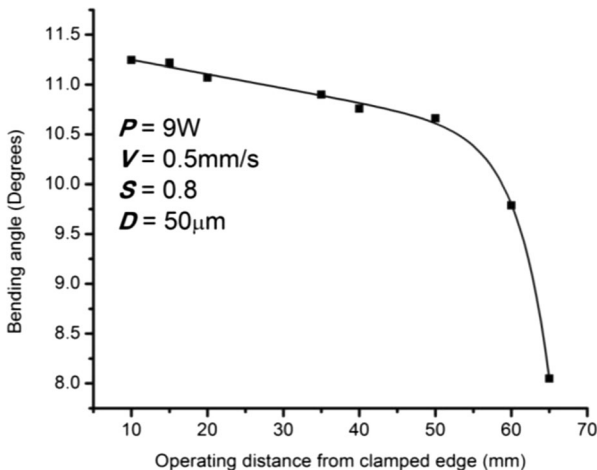


Fig. 8 Effect of operating distance on bending angle

moves closer to the free edge, the amount of mass unaffected by laser heating decreases and hence, lesser internal restraint is generated and lesser bending is achieved.

Effect of Number of Passes on Bending Angle

Multiple laser scans are necessary to obtain the required magnitude of bending angle for most real-life applications. Figure 9 shows the variation of the bending angle with number of passes or laser scans. It can be observed that cumulative bending angle increases almost linearly with the number of scans, with the rate of increase decreasing at higher number of passes, due to work hardening. The extent of work hardening is evident from the graph of incremental bending angle in each pass.

Effect of Number of Passes on *RBAV*

In order to evaluate the variation of bending angle along the free edge, termed as edge effect, bending angle at nine equi-spaced positions along the free edge of the sheet is measured. The edge effect, in terms of relative bending angle variation (*RBAV*), is calculated according to Eq. (2).

$$RBAV = \frac{\Delta\alpha}{\bar{\alpha}} = \frac{\alpha_{\max} - \alpha_{\min}}{\sum_{i=1}^n \alpha_i} \quad (12)$$

RBAV is the relative variation of bending angle, $\Delta\alpha$ is the difference between maximum bending angle (α_{\max}) and minimum bending angle (α_{\min}) along the free edge of the sheet. $\bar{\alpha}$ is the arithmetic average of the bending angles at the equi-spaced sampling points. A low value of *RBAV* is desirable, since it implies a low value of difference between the maximum and minimum bending angle, $\Delta\alpha$ and/or a high value of average bending angle, $\bar{\alpha}$.

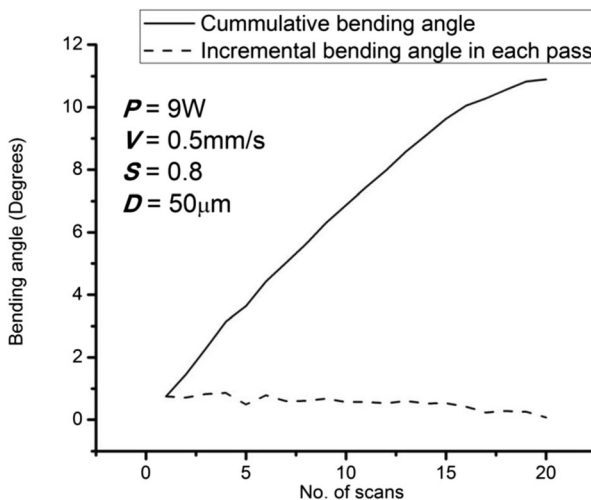


Fig. 9 Effects of number of scan on bending angle

As can be seen from Fig. 10, that with increase in number of laser passes, the average bending angle $\bar{\alpha}$ increases, the difference between the maximum and the minimum bending angle $\Delta\alpha$ first increases and then decreases. The net effect on RBAV is that it decreases monotonically with the number of laser scans.

Comparison of Laser Bending in Terms of Line Energy

Since laser forming process is affected by many factors, it is sometimes advantageous to examine the effect of parameters in a combined way. Line energy is the ratio of power to velocity (P/V). It represents the laser energy input per unit length along the scanning path and it makes sense to consider line energy instead of considering the effects of laser power and scanning speed, separately. The variation of bending angle with line energy is plotted in Fig. 11. The line energy for laser bending is given by $LE_c = P/V$. Figure 11 shows the variation of bending angle with power, for samples scanned with different line energies of 4.5, 6.0, and 9.0 J/mm; spot diameter is kept constant at 50 μm . The plate size is taken as 70 mm \times 40 mm \times 0.8 mm. It is, intuitive to assume that the bending angle achieved will be equal for laser forming with same line energy, despite using different power and velocity combinations. But this has not always been the case. From Fig. 11, it can be seen that the higher the line energy, the larger is the bending angle, because higher line energy results in higher peak

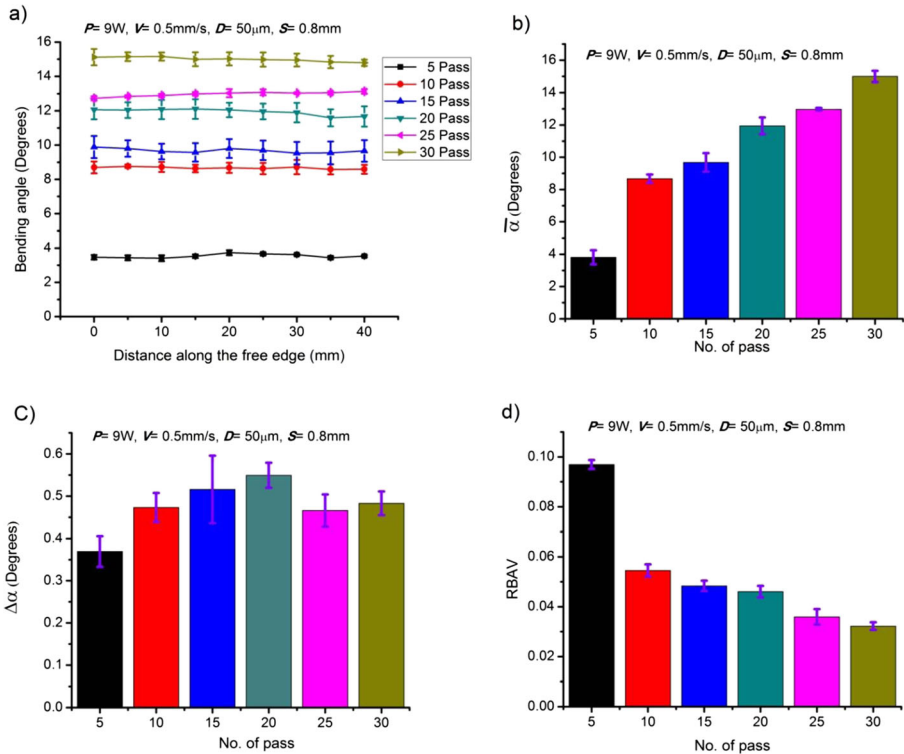


Fig. 10 Effect of number of scans on (a) variation of bending angle along the free edge, (b) average bending angle, (c) difference between maximum and minimum bending angles, (d) relative variation of bending angle

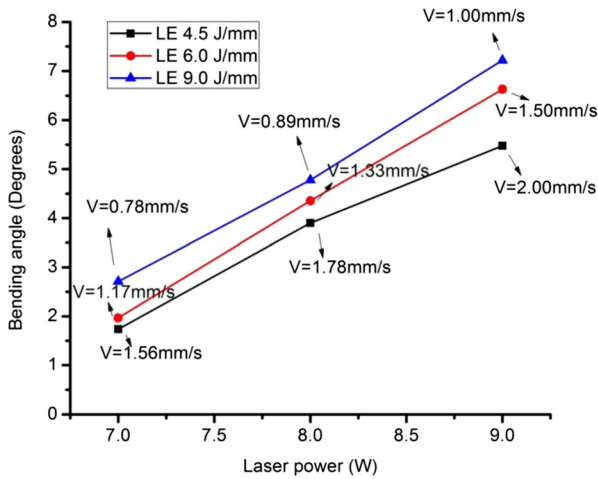


Fig. 11 Variation of bending angle with line energy

temperature on the top surface. Moreover, it can be seen from Fig. 11 that under the condition of constant line energy, the bending angle increases with increase in power (P) and velocity (V). This can also be attributed to the higher peak temperature attained. Even though, the line energy supplied is the same, the parameter (P/V) combination with higher velocity results in higher peak temperature as the loss and diffusion of energy to the surrounding is less as less interaction time is available in this case.

U-Shape Deformation

A plate is subjected to six irradiations on the top surface as shown in Fig. 12a. The plate size is taken as 80 mm \times 40 mm \times 0.8 mm. The scan lines are at a distance of 10, 20, 30, mm, respectively on the left and right sides about the plate centre, at which the plate is fixed in this case. The process parameters are $P = 9$ W, $V = 2.5$ mm/s and $d = 50$ μ m. For each scan line, the number of irradiations is 20. The plate is allowed a cooling time of 12 s between successive scans. The final shape of the workpiece is shown in Fig. 12b.

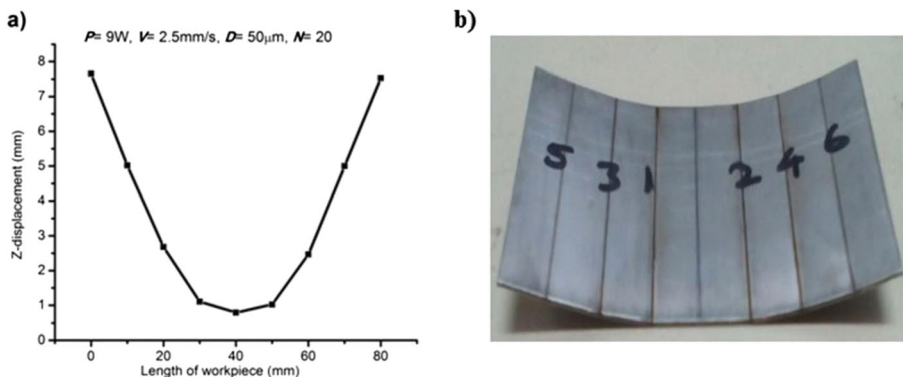


Fig. 12 a Z-displacement after 6 parallel irradiations, b photograph of the laser formed sample

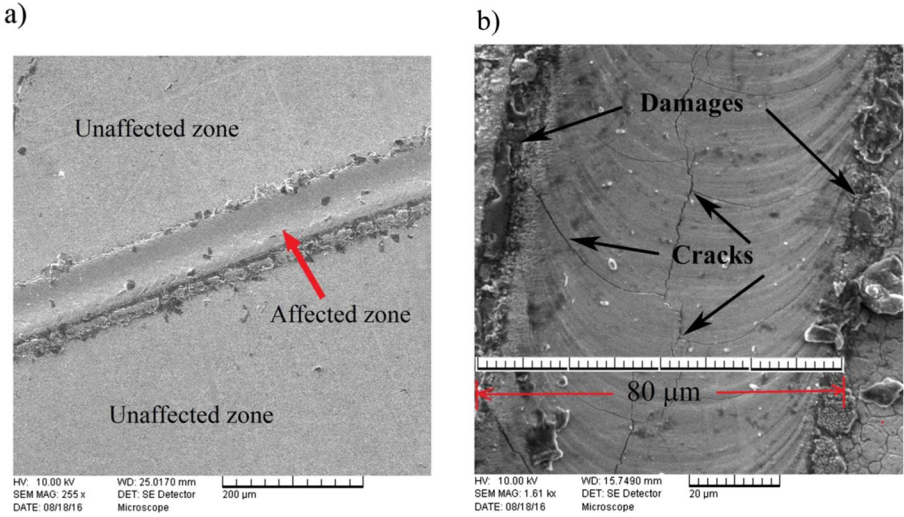


Fig. 13 SEM images of the heat affected zone (a) view of unaffected and affected zones, (b) magnified view of HAZ (laser power = 9 W, scanning speed = 0.5 mm/s, beam diameter = 50 μm)

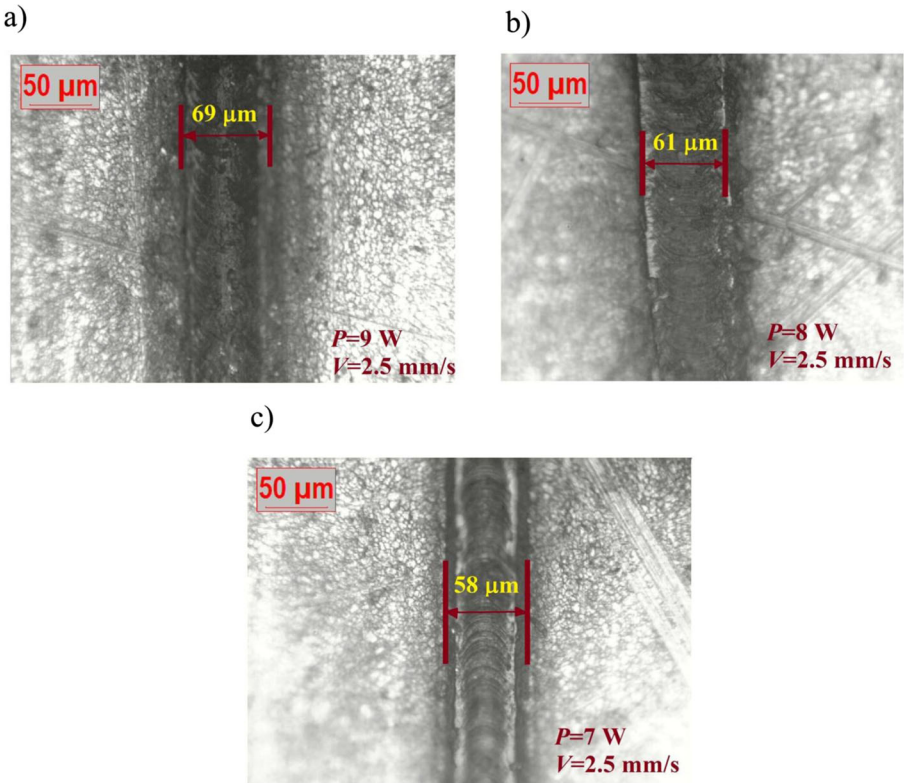


Fig. 14 Surface appearance of the material after 20 number of scans with different power

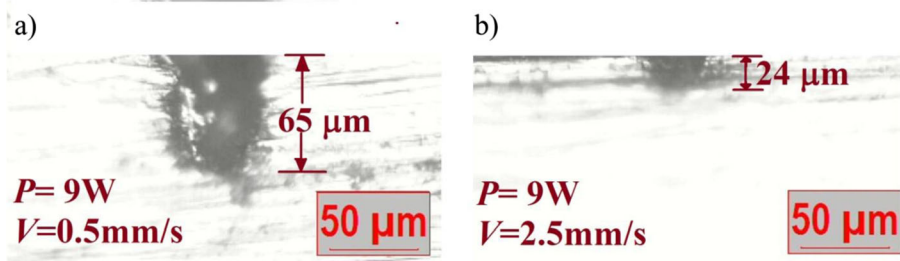


Fig. 15 Surface appearance of the material through plate thickness after 20 number of scans

Heat Affected Zone of AISI 304

A metallurgical investigation is conducted on laser formed AISI 304 specimens to study the effect of laser forming on the micro-structure and heat affected zone (HAZ). Fig 13a, b show the unaffected zone and heat affected zone of AISI 304 after irradiation by Nd:YVO4 laser. From this microstructure, it can be seen that the substrate is damaged over a width of about 80 μm due to the high temperatures experienced during laser forming at a scanning speed of 0.5 mm/s, laser powers of 9 W and beam diameter of 50 μm . The narrow HAZ of about 80 μm for the aforementioned parameters may be attributed to the small diameter of the laser beam.

Figure 14a-c show the effect of laser power on the surface appearance with 20 number of scans. The surface morphology changes occurred due to a high-intensity laser power from a microscopic laser beam diameter. This microscopic diameter of laser beam can cause slight amount of removal of material. The average kerf width observed for the laser powers of 9, 8 and 7 W are 69, 61 and 58 μm , respectively. Figure 15a, b show the influence of scanning speed on the material appearance through the plate thickness with 20 number of scans. The average kerf depth observed for the scanning speeds of 0.5 and 2.5 are 65 and 24 μm , respectively. However, these damages along the width and the depth are very small and can be ignored.

Conclusion

The aim of this experimental study is to identify the effects of process parameters on bending angle of AISI 304 stainless steel sheet using Nd:YVO4 laser. A three dimensional numerical simulation is performed to simulate laser micro-bending. The following conclusions can be drawn from this study based on varying process parameter.

1. The temperature gradient and stress pattern from numerical simulation indicate that bending is caused by temperature gradient mechanism in the present investigation involving laser micro-bending.
2. Bending angle increases with laser power and decreases with increase in scanning speed.
3. Bending angle increases with line energy (LE). Moreover, for the same line energy, a higher bending angle is achieved with higher power (P) and higher scanning speed (V).

4. There is a reduction in bending angle when the operating plane is closer to the free edge.
5. Bending angle increases monotonically with the number of scans. For lower number of pass, the bending angle per pass increases; after a few scans the increment of bending angle decreases with successive scans due to work hardening of the material.
6. Relative variation of bending angle, also called edge effect, decreases significantly when the number of laser pass increases.

References

1. Cheng, P., Yao, Y.L., Liu, C., Pratt, D., Fan, Y.: Analysis and prediction of size effect on laser forming of sheet metal. *Trans N Am Manuf Res Inst SME*. **32**, 439–446 (2004)
2. Venkadeshwaran, K., Das, S., Misra, D.: Bend angle prediction and parameter optimisation for laser bending of stainless steel using FEM and RSM. *Int J Mechatronics Manuf Syst*. **5**(3/4), 308–321 (2012)
3. Hoseinpour, G.M., Mahdavian, S.M., Moslemi, N.H.: Statistical analysis of parameter effects on bending angle in laser forming process by pulsed Nd:YAG laser. *Opt. Laser Technol.* **43**(3), 475–482 (2011)
4. Liu, J., Sun, S., Guan, Y., Ji, Z.: Experimental study on negative laser bending process of steel foils. *Opt. Lasers Eng.* **48**(1), 83–88 (2010)
5. Zahrani, G., Marasi, A.: Experimental investigation of edge effect and longitudinal distortion in laser bending process. *Opt. Laser Technol.* **45**, 301–307 (2013)
6. Shi, Y., Shen, H., Yao, Z., Hu, J.: Temperature gradient mechanism in laser forming of thin plates. *Opt. Laser Technol.* **39**, 858–863 (2007)
7. Walczak, M., Grez, J.R., Celentano, D., Lima, E.B.F.: Sensitization of AISI 302 stainless steel during low-power laser forming. *Opt. Lasers Eng.* **48**, 906–914 (2010)
8. Ojeda, C.V., Grez, J.R.: Bending of stainless steel thin sheets by a raster scanned low power CO₂. *Laser J. Mater. Process. Technol.* **209**, 2641–2647 (2009)
9. Edwardson, S.P., Griffiths, J., Dearden, G., Watkins, K.G.: Temperature gradient mechanism: overview of the multiple pass controlling factors. *Phys. Procedia*. **5**, 53–63 (2010)
10. Chen, G., Xu, X., Poon, C.C., Tam, C.A.: Laser-assisted microscale deformation of stainless steels and ceramics. *Opt. Eng.* **37**(10), 2837–2842 (1998)
11. Zhang, R.X., Xu, X.: High precision microscale bending by pulsed and CW lasers. *J. Manuf. Sci. Eng.* **125**, 512–518 (2003)
12. Zhang, R.X., Xu, X.: Laser bending for high-precision curvature adjustment of micro cantilevers. *Appl. Phys. Lett.* **86**(2), 021114–021113 (2004)
13. Dirscherl, M., Esser, G., Schmidt, M.: Ultrashort pulse laser bending. *J. Laser Micro/Nanoeng.* **1**(1), 54–60 (2006)
14. Ocana, J.L., Morales, M., Molpeceres, C., Garcia, O., Porro, J.A., Garcia-Ballesteros, J.J.: Short pulse laser microforming of thin metal sheets for MEMS manufacturing. *Appl. Surf. Sci.* **254**, 997–1001 (2007)
15. Hu Y., Yao Z., Xu X.: Experimental investigation on the bending deformation of thin 1060 pure aluminum sheet by laser peen forming. Conference proc. international proceeding on shot peening (ICSP-11), September 12–15, 2011, South Bend, Indiana, USA (2011)
16. Griffiths, J., Edwardson, S.P., Dearden, G., Watkins, K.G.: Thermal laser micro-adjustment using picosecond pulse durations. *Appl. Surf. Sci.* **258**, 7639–7643 (2012)
17. Safari, M., Mostaan, H.: Experimental and numerical investigation of laser forming of cylindrical surfaces with arbitrary radius of curvature. *Alex. Eng. J.* **55**, 1941–1949 (2016)
18. Che Jamil, M.S., Sheikh, M.A., Li, L.: A study of the effect of laser beam geometries on laser bending of sheet metal by buckling mechanism. *Opt. Laser Technol.* **43**(1), 183–193 (2011)
19. Venkadeshwaran, K.: Study of laser forming of sheet metal components. Ph.D Thesis, Jadavpur University, Kolkata, India (2012)